Novel three-dimensional MALDI plate for interfacing high-capacity LC separations with MALDI-TOF.

ARTICLE *in* ANALYTICAL CHEMISTRY · DECEMBER 2008

Impact Factor: 5.64 · Source: PubMed

2 AUTHORS, INCLUDING:

Stephen Hattan
Virgin Instruments Corp.
12 PUBLICATIONS **2,758** CITATIONS

Published in final edited form as:
Anal Chem. 2008 December 1; 80(23): 9115–9123.

Novel Three-Dimensional MALDI Plate for Interfacing High-Capacity LC Separations with MALDI-TOF

Stephen J. Hattan* and **Marvin L. Vestal***
Virgin Instruments Corporation, 60 Union Avenue (Suite 1-R), Sudbury, Massachusetts 01776

Abstract

Novel matrix-assisted laser desorption ionization time-of-flight (MALDI-TOF) sample plates employing collimated-hole structures have been developed that allow capture and concentration of samples while simultaneously acting as a sink for carrier solvents. These plates were designed to provide an efficient interface between higher-capacity liquid chromatography (LC) separations and MALDI-TOF mass spectrometry (MS). LC–MALDI using conventional plates can accommodate the low-flow (<1 μL/min) separation protocols typically used in on-line LC–MS methods, and can also be used with higher flow rate, larger columns, but are ultimately limited by the capacity of the two-dimensional surface onto which the sample is deposited. Typically, about 1 μL of chromatographic effluent plus 1 μL of matrix solution can be deposited and dried on a ca. 3 mm diameter spot. Deposition rates (spot dwell time) are determined by the chromatographic resolution and the flow rate. To overcome this limitation, a new three-dimensional MALDI sample plate has been developed using collimated-hole structures (CHS) with monolithic chromatography media filling the holes in the collimated-hole structures. These new plates retain all of the required features of conventional sample plates, commonly formed from stainless steel, but provide additional capacity for capturing and concentrating samples. Results are presented from reversed-phase separation of peptides on a 1 mm i.d. column operating at flow rate of 50 μL/min. Typically, 10 μL of effluent can be collected on a single spot, and sample and matrix dried on a 1 mm diameter spot, to yield about 30-fold enrichment of sample concentration in matrix crystals on the surface compared to the conventional plate. Sample loadings ranging from 1 fmol to 10 pmol/spot were investigated.

Over the past 2 decades mass spectrometry (MS) has emerged as the tool of choice for identifying and quantifying biological analytes (protein, peptides, carbohydrates, lipids, small molecules) in complex biological samples.[1–4] The success of the technique can be attributed to the emergence of new ionization techniques such as electrospray (ESI)[5,6] and matrix-assisted laser desorption ionization (MALDI)[7–9] and by improved MS instrumentation that provides accurate mass and structural information by applying MS/MS techniques.[10–13] A great challenge to large-scale, molecular-level biological investigations (proteomics, glycomics, metabolomics, etc.) is the need to detect and quantify specific analytes from a complex mixture (hundreds to thousands of components) covering a wide range of concentrations.[14,15] It is generally assumed that functional genomics, proteomics, and metabolomics will eventually provide new technologies that revolutionize diagnosis and treatment of disease; however, it is also widely recognized that results toward this end have been slow and that current analytical protocols may not be up to the task.[16–20] The fundamental reason for the difficulty can be simply stated. The range of protein concentrations in biological fluids is very large (potentially 10^{12} for serum[21]), and the dynamic range of the analytical approaches is small (less than 10^3

*To whom correspondence should be addressed. E-mail: stephen.hattan@virgininsturments.com (S.J.H.), marvin.vestal@virgininstruments.com (M.L.V.).

in most cases). Many potentially diagnostic and interesting proteins may be present at very low concentrations (<1 ng/mL). One solution to this problem is to start with enough sample (ca. >1 g of protein) so that low-level protein(s) will be present in adequate quantity for detection and then use extensive fractionate to reduce the probability that these low-level analytes will elute in the same fraction as one at >1000 times higher concentration.

Prior to the development of MALDI, combination of separation techniques with mass spectrometry generally involved on-line direct coupling of the effluent from the chromatograph to the inlet of the mass spectrometer. Techniques such as electrospray, ionspray, and thermospray[22,23] have been employed successfully with a variety of mass spectrometers, including time-of-flight (TOF). The advantage of direct coupling between the separation and the mass spectrometer is that the time scales are the same. But this is also the main disadvantage of direct coupling. All of the measurements on an eluting peak must be made during the time that the peak is present in the effluent. Depending on the speed of the separation technique, this time may be as much as a minute or less than a second. Protein digests derived from complex biological extracts may contain many thousands of peptides in a single sample. Even after liquid chromatography (LC) separation, hundreds of peptides may coelute. Typically, measurements on these digests may involve measurement of the peptide masses in MS mode, deciding which peaks should be measured using MS/MS, and measuring all of the MS/MS spectra of interest. In many cases, the separation must be slowed down to accommodate the speed of the mass spectrometer, or some of the potential information about the sample is lost.[24–26]

To overcome sample complexity, the current trend in on-line LC-MS methodology is toward higher separation efficiency and higher peak capacity, but *lower* sample capacity, nano-LC columns and instrumentation.[27–30] In contrast, the interface between sample separation and MALDI is done off-line. Liquid effluent from separation techniques such as high-performance liquid chromatography (HPLC) or capillary electrophoresis (CE) is mixed postcolumn with a matrix solution and deposited sequentially on a suitable surface and allowed to dry.[7,31,32] The surface containing the dried samples is then inserted into the vacuum system of the MALDI mass spectrometer and irradiated by the laser beam. Off-line coupling has the advantage of allowing sample separation/deposition to occur at a speed appropriate to the chromatography, and the decoupled mass spectrometer can also be operated faster or slower as needed to maximize the information. For example, an entire LC run can be rapidly scanned to determine the peptide mass fingerprints and relative intensities for all peptides in the run. This information can then be used in a true data-dependent manner to set up the MS/MS measurement for all of the spots on the plate to obtain the required information most efficiently.[33,34] In addition, since the sample is essentially locked in place and time by incorporation into the matrix the same run may be iteratively interrogated numerous times until the sample is depleted, something that is rarely realized. A typical spot ~3 mm diameter formed from 10 mg/mL matrix solution can accommodate >100 000 laser shots. The LC–MALDI platform can easily accommodate the low-flow (<1 μL/min) separation protocols typically used in on-line LC–MS methods; currently, it is also compatible with higher flow rate, larger columns with higher capacity for sample loading. Regardless, the primary limitation to further increases in flow rate and sample loading is the two-dimensional surface onto which the sample is deposited. Typically about 1 μL of chromatographic effluent plus 1 μL of matrix solution can be deposited and dried on a ca. 3 mm diameter spot. Deposition rates (spot dwell time) are determined by the chromatographic resolution and the flow rate. Wider chromatography peaks and faster flows lead to an inherent compromise between capturing peaks in a limited number of spots and keeping the spots at a reasonable size (<3 mm). In addition, larger effluent volumes limit the total separation time that can be captured on any given surface. The total capacity of even the new 102 × 108 mm^2 large-format MALDI sample plate is consumed in ~50 min when flowing at 15 μL/min.

To address this problem, a new three-dimensional MALDI sample plate has been developed using collimated-hole structures (CHS) with monolithic chromatography media[27,35,36] filling the holes in the CHS. These new targets retain all of the required features of conventional sample plates, commonly formed from stainless steel, but provide additional capacity for capturing and concentrating samples such as proteins and peptides while acting as a sink for carrier solvents.

EXPERIMENTAL METHODS

Chemicals

ACS-grade styrene, 1-pentanol, 1,4-butandiol, poly(ethylene glycol)-dimethacrylate (PEG-dimethacrylate), 2′,2′-azobisisobutyronitrile (AIBN), α-cyano-4-hydroxy-cinnamic acid (ACCH), trifluoroacetic acid (TFA), acetone, acetonitrile (ACN), water, ethanol, sulfuric acid, nitric acid, ethanethiol, hydrogen peroxide (50%), tech-grade 3,4-dimethoxystyrene, divinylbenzene (DVB), 2-propenethiol, and electrophoresis-grade bovine serum albumin (BSA) were all purchased from Sigma-Aldrich (St. Louis, MO). TPCK-trypsin was purchased from Worthington Biochemical Corp. (Lakewood, NJ).

Plate Construction

Commercially available (Applied Biosystems) 57 × 57 × 1.5 mm^3 and in-house 108 × 102 × 3 mm^3 stainless steel targets were machined with through-holes to form the CHS substrate that housed the monolithic material. The work discussed here was done on a 10 × 10 array of 2.5 mm diameter holes with 3.175 mm spacing on the commercial target or a 27 × 25 rectangular array of 3-to-1 mm tapered holes on the in-house target. Postmachining, plates are cleaned by the following procedure: rinse with H_2O; soak in piranha solution (H_2SO_4/H_2O_2 (3:1)) 0.5 h; rinse with H_2O; soak with 20% HNO_3 3 h; rinse with H_2O and air-dry. Postcleaning, plates are soaked (3 h) in a thiol solution composed of (w/w) 5% 2-propenethiol and 5% ethanethiol dissolved in ethanol. Plates are then rinsed with ethanol and allow to air-dry. Degassed monomer-liquor (w/w 15% styrene, 15% DVB, 5% PEG-dimethacrylate, 5% dimethoxystyrene, 42% 1-pentanol, 18% 1,4-butandiol, 0.25% AIBN) is pumped through a port on the bottom of a tetrafluoroethylene mold capped with aluminum plates to completely fill the mold with solution exiting through a port in the top. Once full, the chamber is pressurized (~50 psi), sealed, and placed in an oven (60 °C) to thermally initiate a free radical polymer chain reaction. In the oven, the reaction chamber is placed on a horizontal spindle and slow rotated to minimize the development of thermal and/or density gradients throughout the course of the reaction.

The steps involved in plate construction are illustrated in Figure 1. After the reaction is completed the mold is opened as illustrated in Figure 1A. Excess polymeric material is removed manually by shaving the polymer with a razor blade until the polymer in the holes is coincident with the metal surface as shown in Figure 1B. Figure 1 illustrates the construction of a 57 × 57 × 1.5 mm^3 CHS plate containing a 5 × 5 array of 3 mm holes. A number of CHS plates with different dimensions, different hole arrays, and hole geometries have been made using this procedure for construction.

LC Interface

An interface module was developed that allows LC effluent to be deposited on either conventional MALDI plates or on CHS plates. The apparatus includes *x*–*y* positioning of deposition with a precision of <50 μm. A solenoid lift provides *z*-axis motion as needed. The exit from the LC column is coupled to the interface via a 40 cm length of 150 μm i.d. PEEK tubing. For deposition on conventional plates the tip of the PEEK tube is located ca. 0.5 mm from the plate, and liquid flows onto the plate. After a predetermined deposition time the tip

is lifted by actuating the solenoid, the tip is quickly moved to the next location (ca. 0.1 s), lowered to the deposition distance, and the next spot deposited. For deposition on CHS plates, the lift mechanism is disabled and the tip is sealed to the sample plate using a spring-loaded coupling.

Sample Elution

The elution apparatus used for all CHS targets is shown in Figure 2. As shown, the large-format plate is in the elution position. The syringe pump is manually adjusted to control pressure on a reservoir of matrix solution located under the plate. The analytical side of the plate is visually monitored through the clear acrylic chamber, and the exhaust fan attached to the chamber is used to assist matrix solution evaporation and consequent matrix crystal formation. The housing used for eluting the 57 × 57 mm^2 plates is show at the top of the apparatus. Sample elution on CHS plates occurs from all holes simultaneously. With the use of the apparatus shown in Figure 2, dilute MALDI matrix solution (2 mg/mL ACCH, 56% ACN, 25% acetone, 19% H_2O, 0.1% TFA) is forced through the plate in sufficient volume to adequately wash bound analyte back to the plate surface where it is allowed to dry and is incorporated into the matrix crystals. The elution process is controlled by visually monitoring the matrix solution as it emerges on the top or analytical side of the plate and then manually adjusting the syringe pump so that elution and evaporation are balanced to prevent solvent pooling between adjacent spots. Typical elution flows range from between 0.4 and 1 μL/min/hole depending on geometry, and the total volume passed through a given plate was 4× the estimated individual-hole void volume multiplied by the total number of holes. For example, for the large-format 675 well plate the void volume per hole was estimated at 5 μL (based on 50% polymer occupancy); therefore 5 × 675 × 4 = 13 500 or 13.5 mL of elution solvent was used.

Liquid Chromatography

Chromatography was accomplished using binary solvent, gradient elution on an Eldex MicroPro syringe pumping system (solvent A = 5% ACN, 0.1% TFA; solvent B = 85% ACN, 5% isopropyl alcohol (IPA), 0.1% TFA). The 15 μL/min separations were performed on a 10 mm × 0.5 mm, 3 μm, 200 Å, C-18 column (Eksigent) using gradient of increasing percent B over the following time intervals: 5–12% B 5 min, 12–35% B 40 min, 35–90% B 15 min at T = 42 °C. The 50 μL/ min separations were performed on 50 mm × 1 mm, 5 μm, 200 Å, C-18 column (Higgins Analytical) using gradient of increasing percent B over the following time intervals: 5–12% B 2 min, 12–45% B 23 min, 45–90% B 3 min at T = 42 °C. An elevated column temperature was used to decrease peptide retention for the C-18 column in order to foster peptide elution at lower organic phase compositions. This step was taken to help ensure that peptides eluting from the C-18 resin would still have affinity for the less hydrophobic monolithic polystyrene resin contained within the CHS plates. In addition, the CHS plates were saturated with solvent A prior to LC separation so the LC effluent, upon entering the CHS plate, would also undergo a subtle dilution in its organic phase content.

Gold Coating

Gold sputter-coating of the 57 × 57 CHS target was used to create a thin, conductive layer as a preventive measure against surface charging of the polymer during MALDI-TOF analysis. An MTK-600 L-13 system (Manitou Systems Inc.) using argon process gas (application pressure 10 Torr) and rf forward power of 65 W was used to sputter a thin layer (~150 Å) of gold at 15 cm distance. The system is equipped with a rotating stage, and total sputter time per plate was 3 min.

Mass Spectrometry

Initial mass spectrometry studies were performed on an early prototype of the AB4700 (Applied Biosystems, Framingham, MA). This instrument employs the 57 × 57 × 1.5 mm^3 stainless steel plates employed in all of the Voyager series of MALDI-TOF mass spectrometers from ABI. The CHS plates used in the fundamental work were based on this format. A new series of high-performance MALDI-TOF MS and MS/MS instruments are currently under development, and initial results on the design and performance of these instruments were recently described.[45] These instruments employ a larger plate format of 127 × 124 × 3 mm^3 with an active area 102 × 108 mm^2. Adaptors are available that allow standard microplates (72 × 108 mm^2) or up to four of the small-format plates to be loaded and analyzed in the new instruments. Initial fundamental studies employed the smaller format plates with the prototype AB4700 mass spectrometry (Figure 3 and Figure 4), and the work on interfacing directly with LC separation at higher flow rates has employed the larger format plates with a new high-resolution MALDI-TOF instrument.[45]

RESULTS AND DISCUSSION

Figure 3 shows plots of signal intensity resulting from a “high-density” plate surface analysis of a 1 pmol separation of a BSA digest performed at 15 μ/min flow. For “high-density” surface scans, such as those shown in Figure 3, acquisitions were performed at 0.5 mm intervals in a 60 × 60 array, and all other plate scans were performed by single acquisitions centered on each location of the 10 × 10 array of collimated holes. MS acquisitions typically accumulated signal from 2000 laser shots (200 Hz) averaged from 80 sample positions (“search pattern positions”), and spectra were recorded over a 300–2500 Da mass range.

Figure 3A shows the extracted ion chromatogram (EIC) for all masses in the range of 900–2400, and the plot shows that multiple peaks from the digest have been captured and preserved by the CHS plate. Figure 3B shows data from the same run; however, this time the plot is an overlay of three EICs done on individual peptides within the digest. Figure 3B shows that the individual peptides have discreet locations and that even running at flow rate of 15 μL/min and a dwell time of 30 s/spot the CHS plate is able to capture these peptides while preserving chromatographic resolution. Figure 3C shows the EIC of mass 379 which corresponds the dimer peak of the ACCH matrix. Figure 3C is shown to demonstrate the reasonably even distribution of matrix across the plate surface.

Table 1 and Table 2 list the integrated peak areas for 12 of the more abundant peptides detected in the analyses of BSA digest. Table 1 shows data extracted from LC separations of an identical BSA sample performed multiple times on the same CHS plate. Between runs the plate was simply washed with several volumes of elution solvent (minus matrix) prior to reuse. Table 2 shows data extracted from LC separations of an identical BSA sample performed on three different CHS plates. Although the variation in signal intensity is different for the different peptides the average standard deviation in signal intensity in both cases is ~20% (18.46 and 21.39). The peak areas presented in the tables are raw data that has not been normalized to the signal intensity of a standard (as is often done for quantitation by MALDI).

For a given set of experimental conditions (solvent formulation, temperature, etc.), the peptide binding capacity of any hole on a CHS plate depends on the chemical and physical constitution of the polymer and the hole dimensions. In order to estimate the capacity for the monolith used here, a loading study was conducted on our in-house plate. Two different loading scenarios where investigated. The first tested the binding capacity of the monolith, and the second tested the approximate dynamic range of measurement that the CHS plate is capable of achieving. Results from the study are shown in Figure 4 along with accompanying Table 3 and Table 4. The binding capacity was determined by loading samples to ensure that the void volume of the

individual holes was exceeded. Once the threshold of binding for the polymer had been exceeded, excess sample passes through the hole resulting in no measured increase in signal. Figure 4A shows a plot of 3 dilutions of a BSA digest (5, 50, 500 fmol/μL) that were loaded for different times increments to achieve volumes of 5, 10, 15 μL to cover a range of 25–7500 fmol in quantity. As the plot in Figure 4A shows, there is a nearly linear increase in the measured signal intensity for the 1300–2400 Da peptide mass range up to about 2500 fmol; further loading results in no signal increase. The data presented in Figure 4A is summarized in Table 3. Figure 4B shows a second loading study wherein the void volume of the holes was *not* exceeded. This was done by varying the sample concentration and keeping the load volume constant to cover a range of 25–10 000 fmol in quantity. Figure 4B shows that without exceeding the void volume of holes the dynamic range of plate can be extended ~3?×. This is not unexpected because, even after saturation of the polymer binding capacity, excess peptide will remain trapped in the confines of the hole and can be eluted to the surface and incorporated into the matrix in a manner that is indistinguishable from adsorbed peptide. It is hypothesized that the drop in signal intensity at loadings of above 7.5 pmol is caused by there being too much analyte (not enough matrix) for efficient ionization of the entire sample. The data presented in Figure 4B is also shown in Table 4.

Figure 5 presents results from a comparative study of a sample spotted on a CHS plate versus a two-dimensional (2D) stainless steel plate (SS). This comparison was done using the identical sample (100 fmol of BSA digest), identical LC separation conditions, 15 μ/min flow, and identical operating conditions for the MALDI MS. The separation conditions were chosen because they approximate the maximum flow rate that can be effectively spotted on the 2D 108 × 102 mm^2 SS plate in ~1 h. Direct LC deposition on a 2D plate allows for maximum droplet volume of ~2.5 μL for a 2.5–3 mm spot, and matrix solution is added postcolumn further reducing the volume of chromatographic effluent per spot to about 1.25 μL. Therefore, with a column flow of 15 μL/min, a spotting rate of 12 spots/min is required to avoid flooding the plate, and a 56 min chromatogram can be recorded to provide 675 spots in a 27 × 25 matrix with 4 mm spacing. With the use of the same 675 spot format on the CHS plate, a sampling frequency of 30s/hole was used to capture and concentrate the eluting peaks, and postelution a spot diameter 1.2 mm was realized. It is important to note that at this sampling rate a 1 h separation may be captured in ~100 wells and, as such, five runs of ~1 h each can be recorded on a single plate. Figure 5 shows the selected ion chromatograms across the entire plate (lower panel) for the most intense ion in the BSA spectrum (1479.80) along with the mass spectrum and a blow up of the region of interest for the most intense location on the plate for the CHS plate (Figure 5A) and SS plate (Figure 5B). The intensity scales for each chromatogram correspond to the integrated ion intensity over the isotopic envelope for the selected ion. With MALDI, relative signal intensities can depend on other factors in addition to surface concentration of sample; however, by comparing the strength of a given signal with that of an internal standard in the matrix solution, it is possible to determine a more quantitative response. Figure 6 shows an expanded view of the EIC of 1479. The signal intensities in the upper panel show that, based the ratio of the raw peak intensities, an increase of ~13× is achieved by using the CHS plate; however, when the intensities are calibrated relative to the 1045.29 reference peak, an intensity increase of 32× is realized. The nominal sample concentration on the surface at the maximum intensity is inversely proportional to the spot area and the sampling rate. Therefore, with an ~6× lower sampling frequency and an ~6× smaller spot area, a 36× signal enhancement is expected on the CHS plate in comparison to the SS plate; the experimental result is in good agreement with this value, indicating nearly 100% sample recovery.

This comparative study was conducted at a 15 μL/min flow because it approximates the maximum practical flow rate for sample collection on a 2D surface over a 1 h time frame, and even this is only possible due to the increased surface area afforded by the 127 × 124 mm^2

MALDI target. However, CHS plates can easily accommodate higher flows without sacrificing performance.

Figure 7 shows the results of four serial separations of 5 pmol of BSA digest run at a 50 μL/min flow spotted on a single 108 × 102 large-format CHS plate. The plot shows the overlay of the EIC for 12 peptides (chosen for their approximate similar intensities) plotted as a function of location. The EIC intensities in Figure 7 were normalized relative to *m*/*z* 1045.29 standard that was added to the matrix solution at a 100 fmol/μL concentration prior to sample elution. Inclusion of an internal mass standard is useful for instrument mass calibration but is also useful for inter-run comparisons as variable signals can be normalized relative to the intensity of the standard that is present in equal quantity at all locations. Figure 7 not only demonstrates effective operation at a flow rate 50–100× higher than most current LC–MS and LC–MALDI experimental protocols but also the reasonable reproducibility across ~4 h of chromatography captured on a single plate. Statistical information for the peaks shown in Figure 7 is included in Table 5. Success of CHS plates depends on uniformity in the structure and performance of the capture media contained within the individual holes. Monolithic column technology was attractive because construction (like polyacrylamide gel electrophoresis (PAGE) gel construction) begins with the reactive monomers dissolved in a miscible solvent composing a homogeneous solution that can be pumped into empty CHS plates, formatted in any configuration, for even and complete filling. Second, polymer formation takes places inside the holes and allows for surface chemistry to be used to achieve covalent attachment of the polymer to the inner walls of the collimated holes. Thiol compounds used for the creation of a self-assembled monolayer (SAM)[37–39] were utilized for this purpose. Cleaned plates were soaked in thiol solution of 2-propenethiol to create this covalent link between the polymer and the metal. Ethanethiol was also added to the mixture as a spacer to help guard against the potential propagation of polymerization between adjacent propenethiol groups on the metal surface. Initially, prior to SAM formation the cleaned plates were sputter-coated with a thin layer of gold; however, comparative examination on plate stability proved this step to be unnecessary. Third, the resulting polymer forms a single, cross-linked, continuous structure that contains a network of through-pores, the size of which can be controlled by the choice/concentration of the monomer(s) and dilution solvent(s) (porogens) that make it liquid-permeable. This means that not only can different polymers be used for different modes of analyte capture (reversed-phase, ion-exchange, affinity binding) but, also, that any given polymer may have its formulation tuned to adjust physical parameters such as pore size to achieve high or low resistance to flow or to optimize the pores to target different sized molecules (protein, peptide, small molecule). For example, the peptide capture experiments discussed here use a monolith formulated in pentanol because it was determined best for this application. However, thicker (10 mm), higher-capacity plates have been constructed for protein capture using propanol to allow for larger pores and easier flow through the thicker plate (data not shown).

Current LC-MALDI protocols typically spot sample directly onto the surface of SS targets and, therefore, are limited to ~2.5–3 μL total volume for effective spotting of optimally sized spots and are thus limited to separations that operate efficiently at flow rates of ~2 μL/min. Although targets like the anchor-chip[40] and μFocusplate[41] have been developed that make use of surface chemistry to focus deposited liquid volumes into a confined area and, in doing so, effectively increase the surface concentration of analytes, these devices suffer the same limitation and ceilings regarding manageable effluent volumes as ordinary SS plates under typical LC-MALDI conditions. The “integrated selective enrichment target” (ISET)[42,43] technology is conceptually similar to CHS plates in that microwells cut into the MALDI target are filled with beaded resin(s) for the selective capture of analyte, and other devices such as the surface mask[44] attached on top of a MALDI target to create an effective liquid fraction collector on the plate surface (~200 μL/well) have been efficiently coupled to higher flow protein

separations. However, these systems differ from the CHS plates in that, in the case of ISET, the wells house loose beaded resins that are not incorporated into the plate substrate and plates have not been demonstrated as being successfully coupled to LC, and regarding the affixed mask, there is no capture media or resin, and postseparation, the collected liquid effluent is dried in a Speed-Vac in order to concentrate the sample to the target surface. Although the strategies mentioned above are highly regarded and represent excellent examples of characteristics inherent to the LC–MALDI analytical platform that can be exploited advantageously, the CHS plates described here draw from different aspects of each these strategies with designs to improve and expand the capabilities of the LC–MALDI technique.

CONCLUSION

CHS MALDI plates with monolithic structures have been demonstrated to successfully couple LC separations to MALDI MS with 100× the sample loading capacity and operating under LC conditions that quickly overwhelm the capabilities of typical 2D targets. Although the ultimate sample capacity of a given CHS plate depends on the monolith used, the plate geometry, the sample, and the loading conditions, plates used in this study were determined to have a binding capacity of ~2.5 pmol/hole of digested BSA protein (~0.17 μg/hole based on a protein MW = 66 430) and an ~7.5 pmol/hole (~0.50 μg/hole) quantity of total capture. A large-format CHS plate was used to demonstrate the reproducible capture and elution of four serial chromatographic separations run at a 50 μL/min flow rate and spanning 4 h of chromatographic time on a single plate. Since the collimated holes act as a sink for chromatographic carrier solvents the dwell time per spot can be varied over a wide range to match the chromatographic performance. Controlled elution of all holes simultaneously with a matrix-containing elutant is used to bring the trapped sample back to the surface with quantitative efficiency where it becomes incorporated into matrix crystals and is analyzed directly. Individual targets have been demonstrated as reusable with reasonable reproducibility, and this is expected to be similar to chromatography columns generally. A minor problem with early designs was that the best sensitivity was obtained when the matrix crystals formed within the diameter of the upper hole on the surface of the monolithic polymer. Unfortunately, the polymer is an insulator and some loss in resolution and mass accuracy resulted from surface charging. This can be overcome by sputtering a thin layer of gold on the surface to act as a conductive layer. Although this is a practical solution for the feasibility studies it adds significant expense and complexity the overall scheme; however, the newer, tapered-hole design used in the large-format plate has reduced the problem to only slight loss (~20%) in resolution in the absence of gold coating. Except for this small loss in resolution there appear to be no significant differences between crystals formed on the surface of the polymer and those on the metal surface. Although detailed studies have not been done, we see no obvious evidence of differences in either ionization efficiency or number or laser shots/spot for sample depletion. The tapered design has the additional benefit of confining eluted sample into a small area leading to a more concentrated sample on the analytical surface and eventually to higher overall analytical sensitivity. A new approach to construction of the plates employs photoetching techniques that may allow the area of exposed polymer on the surface exposed to the laser to be further reduced to approximately that of the laser beam. This may make the effect of surface charging insignificant, thus removing the need for gold sputtering and further reducing the size of the sample spot.

Acknowledgments

Recognition and thanks are deserved for the entire Virgin Instruments staff for significant contributions to this project: Christina Vestal, Kevin Hayden, Roger Voyer, Joseph Fitzpatrick, George Mills, Matthew Gabeler-Lee, Steve Gabeler, Mark Dahl, and Joseph Valentine. Funding for this work was provided by SBIR Grant GM079833.

References

1. Celis JE, Korc M. Mol. Cell. Proteomics 2005;4:345–598.
2. Goodacre R. Metabolomics 2005;1:1–2.
3. Kussmann M, Raymond F, Affolter M. J. Biotechnol 2006;124758-539
4. Powell DW, Merchant ML, Link AJ. Expert Rev. Proteomics 2006;3:63–74. [PubMed: 16445351]
5. Fenn J, Mann M, Meng CK, Wong SF. Science 1989;246:64–71. [PubMed: 2675315]
6. Kebarle P, Tang L. Anal. Chem 1993;65:972A–986A.
7. Karas M, Hillenkamp F. Anal. Chem 1988;60:2299–2301. [PubMed: 3239801]
8. Tanaka K, Hiroaki W, Yutaka I, Satoshi A, Yoshikazu Y, Tamio Y, Matsuo T. Rapid Commun. Mass Spectrom 1988;2:151–153.
9. Martin SA, Biemann KA. Int. J. Mass Spectrom. Ion Processes 1987;78:213–228.
10. Yost RA, Enke CE. J. Am. Chem. Soc 1978;100:2274–2275.
11. Vestal, ML.; Juhasz, P.; Hines, W.; Martin, SA. Mass Spectrometry in Biology and Medicine. Totowa, NJ: Humana Press; 2000. p. 1-16.
12. Morris HR, Paxton T, Dell A, Langhorne J, Berg M, Bordoli RS, Hoyes J, Bateman RH. Rapid Commun. Mass Spectrom 1996;10:889–896. [PubMed: 8777321]
13. Cody RB, Frieser BS. Anal. Chem 1982;54:1431–1433.
14. Veenstra TD, Conrads TP, Hood BL, Avellino AM. Mol. Cell. Proteomics 2005;4:409–418. [PubMed: 15684407]
15. Ackermann BL, Hale JE, Duffin KL. Curr. Drug Metab 2006;7:525–539. [PubMed: 16787160]
16. Chen G, Pramanik BN. Expert Rev. Proteomics 2008;5:435–444. [PubMed: 18532911]
17. Panchaud A, Affolter M, Moreillon P, Kussmann M. J. Proteomics 2008;71:19–33. [PubMed: 18541471]
18. Briscoe CJ, Stiles MR, Hage DS. J. Pharm. Biomed. Anal 2007;44:484–491. [PubMed: 17433601]
19. Garbis S, Lubec G, Fountoulakis M. J. Chromatogr., A 2005;1077:1–18. [PubMed: 15988981]
20. Omenn G. Proteomics 2004;4:1235–1240. [PubMed: 15188391]
21. Lundblad RL. Internet J. Genomics Proteomics 2005;1(No 2)
22. Vestal ML. Science 1984;226:275–281. [PubMed: 6385251]
23. Tomer KB. Chem. Rev 2001;101:297–328. [PubMed: 11712249]
24. Li F, Maguigad J, Pelzer M, Jiang X, Ji QC. Rapid Commun. Mass Spectrom 2008;22:486–494. [PubMed: 18215007]
25. Davis MT, Stahl DC, Hefta SA, Lee TD. Anal. Chem 1995;67:4549–4556. [PubMed: 8633788]
26. Vissers JP, Blackburn RK, Moseley MA. J. Am. Soc. Mass Spectrom 2002;13:760–771. [PubMed: 12148801]
27. Ivanov AR, Zang L, Karger BL. Anal. Chem 2003;75:5306–5316. [PubMed: 14710807]
28. Stutz H. Electrophoresis 2005;26:1254–1299. [PubMed: 15776483]
29. Shen Y, Zhao R, Berger SJ, Anderson GA. Anal. Chem 2002;74:4235–4249. [PubMed: 12199598]
30. Wolters DA, Washburn MP, Yates JR III. Anal. Chem 2001;73:5683–5690. [PubMed: 11774908]
31. Beavis RC, Chait BT. Rapid Commun. Mass Spectrom 1989;3:233–237. [PubMed: 2520242]
32. Hattan SJ, Marchese J, Albertinetti M, Krishnan S, Khainovski N, Juhasz P. J. Chromatogr., A 2004;1053:291–297. [PubMed: 15543995]
33. Graber A, Juhasz P, Khainovski N, Parker K, Patterson DH, Martin SA. Proteomics 2004;4:474–489. [PubMed: 14760720]
34. Hattan SJ, Parker KC. Anal. Chem 2006;78:7986–7996. [PubMed: 17134131]
35. Xie S, Allington RW, Svec F, Frechet JMJ. J. Chromatogr., A 1999;865:169–174. [PubMed: 10674939]
36. Svec F, Huber C. Anal. Chem 2006;78:2100–2107.
37. Witt D, Klajn R, Barski P, Grzybowski BA. Curr. Org. Chem 2004;8:1763–1797.
38. Ulman A. Chem. Rev 1996;96:1533–1554. [PubMed: 11848802]

39. Poirier G. Chem. Rev 1997;97:1117–1127. [PubMed: 11851444]
40. Schuerenberg M, Luebbert C, Eickhoff H, Kalkum M, Lehrach H, Nordhoff E. Anal. Chem 2000;72:3436–3442. [PubMed: 10952524]
41. Gobom J, Schuerenberg M, Mueller M, Theiss D, Lehrach H, Nordhoff E. Anal. Chem 2001;73:434–438. [PubMed: 11217742]
42. Eckström S, Wallman L, Hellin G, Nilsson J, Marko-Varga G, Laurell T. J. Mass Spectrom 2007;42:1445–1452. [PubMed: 17960572]
43. Eckström S, Wallman L, Malm J, Becker C, Lilja H, Laurell T, Marko-Varga G. Electrophoresis 2004;25:3769–3777. [PubMed: 15565686]
44. Perlman DH, Huang H, Dauly C, Costello CE, McComb ME. Anal. Chem 2007;79:2058–2066. [PubMed: 17256876]
45. Vestal ML, Hayden K. Int. J. Mass Spectrom 2007;268:83–92.

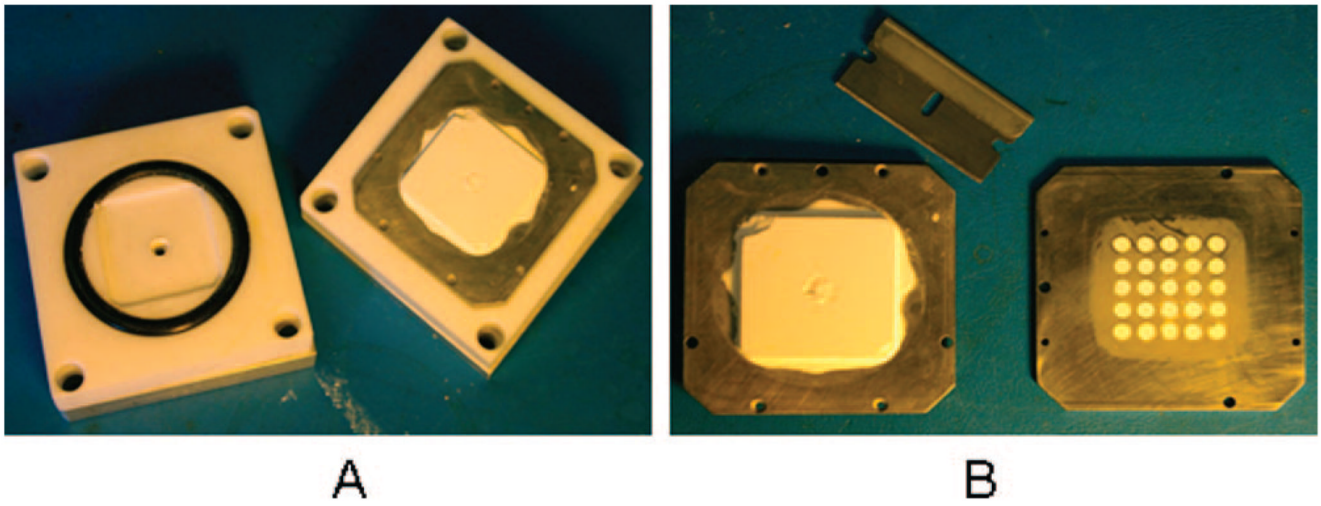

Figure 1.
Reaction chamber and postpolymerization process used to construct CHS plates.

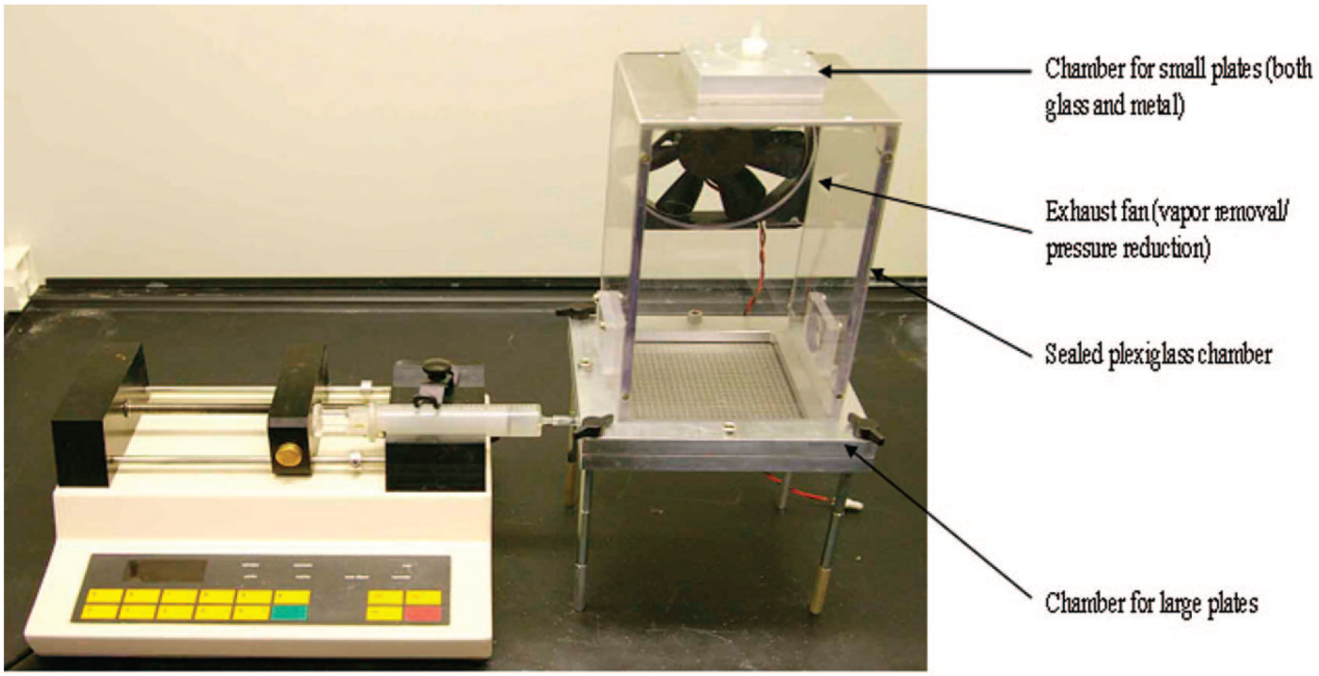

Figure 2.
Elution apparatus used for sample elution and matrix crystal formation.

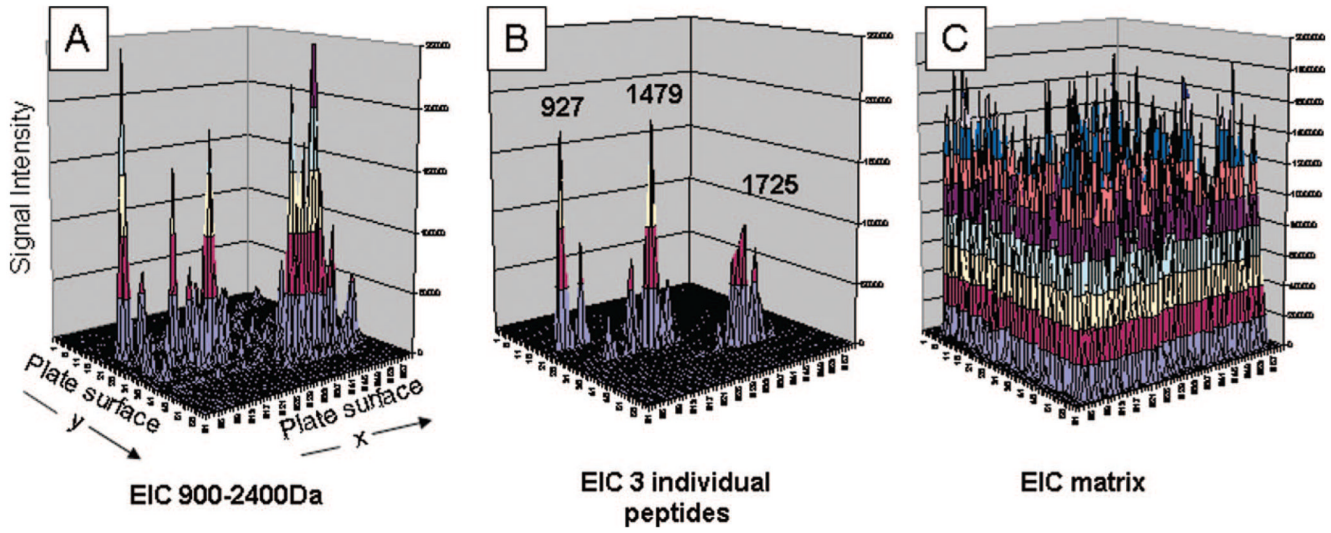

Figure 3.

"High-density" MS surface analysis of a 10 × 10 array CHS plate after capture and elution of 1 pmol of BSA digest LC separation. Frame A: extracted ion chromatogram (EIC) of the 900–2400 mass range. Frame B: overlay EIC for three individual peptides. Frame C: EIC of the 379 Da ACCH matrix dimer.

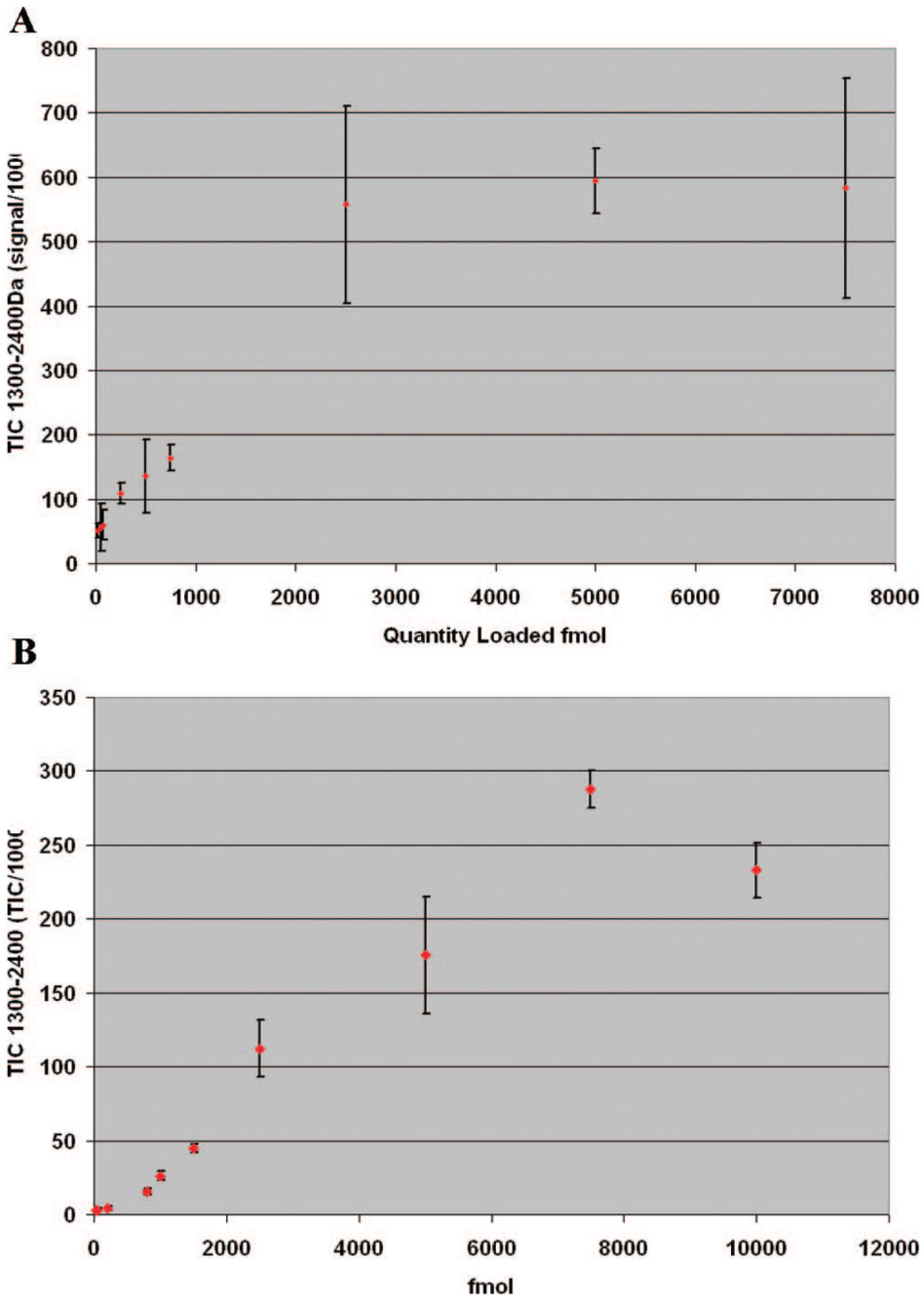

Figure 4.

(A) Plot of concentration vs EIC (1300–2400 Da) for different loadings of BSA digest done so that the void volume of the individual collimated holes was exceeded. *N* = 8 for all data points. (B) Plot of concentration vs EIC (1300–2400 Da) for different loadings of BSA digest done so that the void volume of the individual collimated holes was not exceeded. *N* = 8 for all data points.

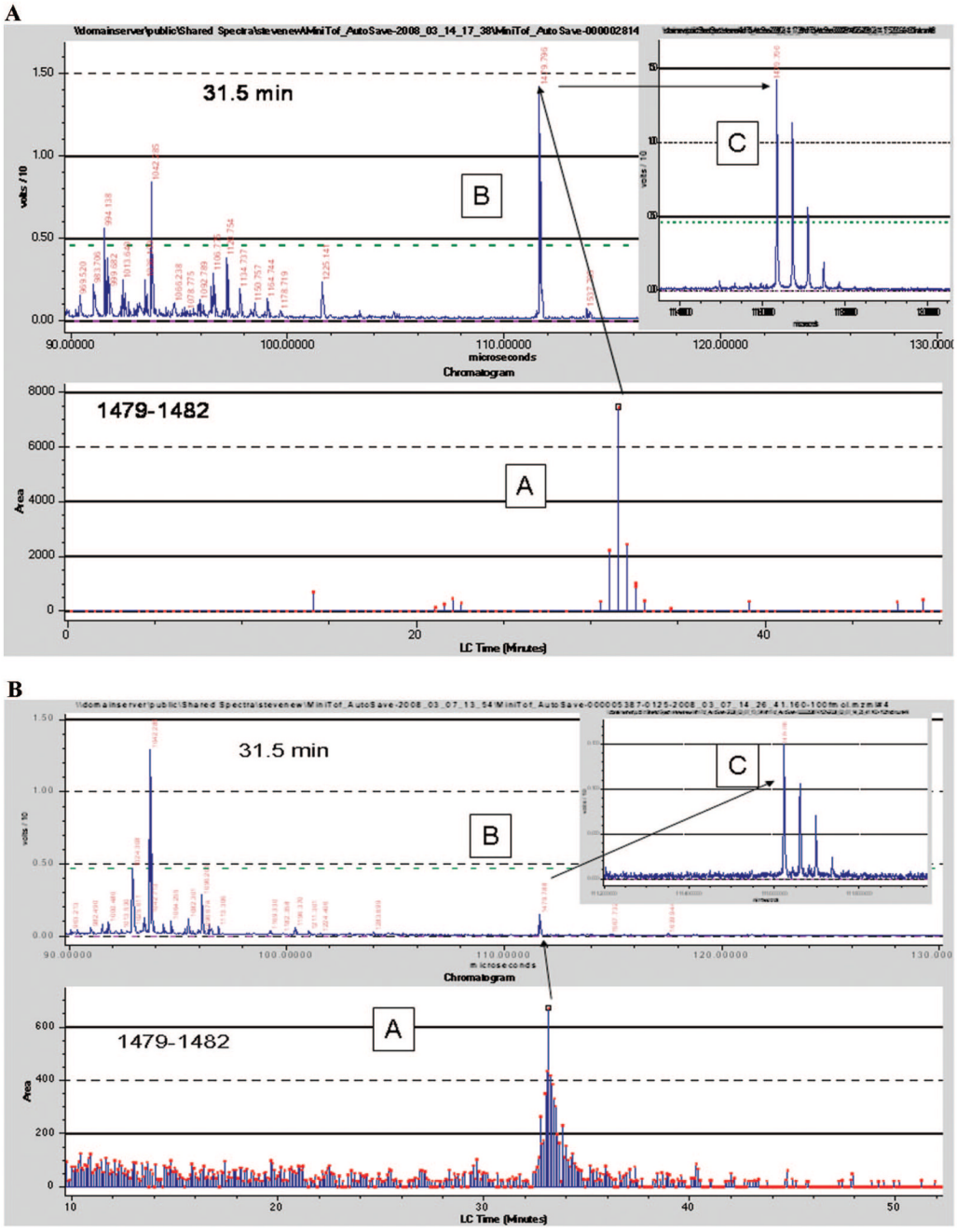

Figure 5.

(A) Extracted ion chromatogram of mass 1479.80 Da from a CHS plate (A), mass spectra from the spot of maximum intensity (B), and blow-up of the region of interest (C). (B) Extracted ion chromatogram of mass 1479.80 Da from a SS plate (A), mass spectra from the spot of maximum intensity (B), and blow-up of the region of interest (C).

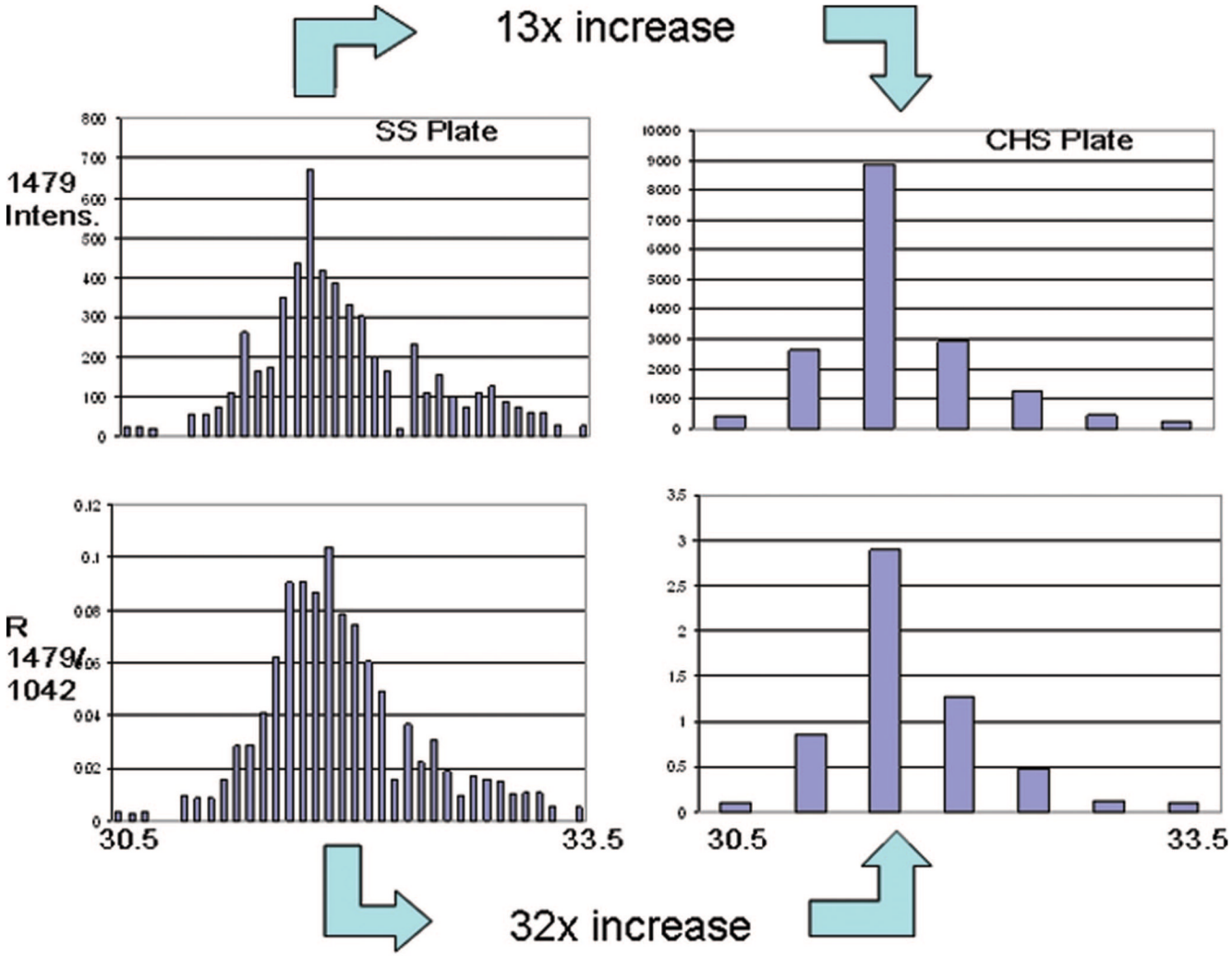

Figure 6.
Blow-up of the extracted ion chromatogram of 1479.80 shows an ~13× increase in raw peak intensity achieved by using the CHS plate (upper set of panels); however, when the intensities are compared relative to the 1045.29 reference peak, an intensity increase of 32× is realized (lower set of panels).

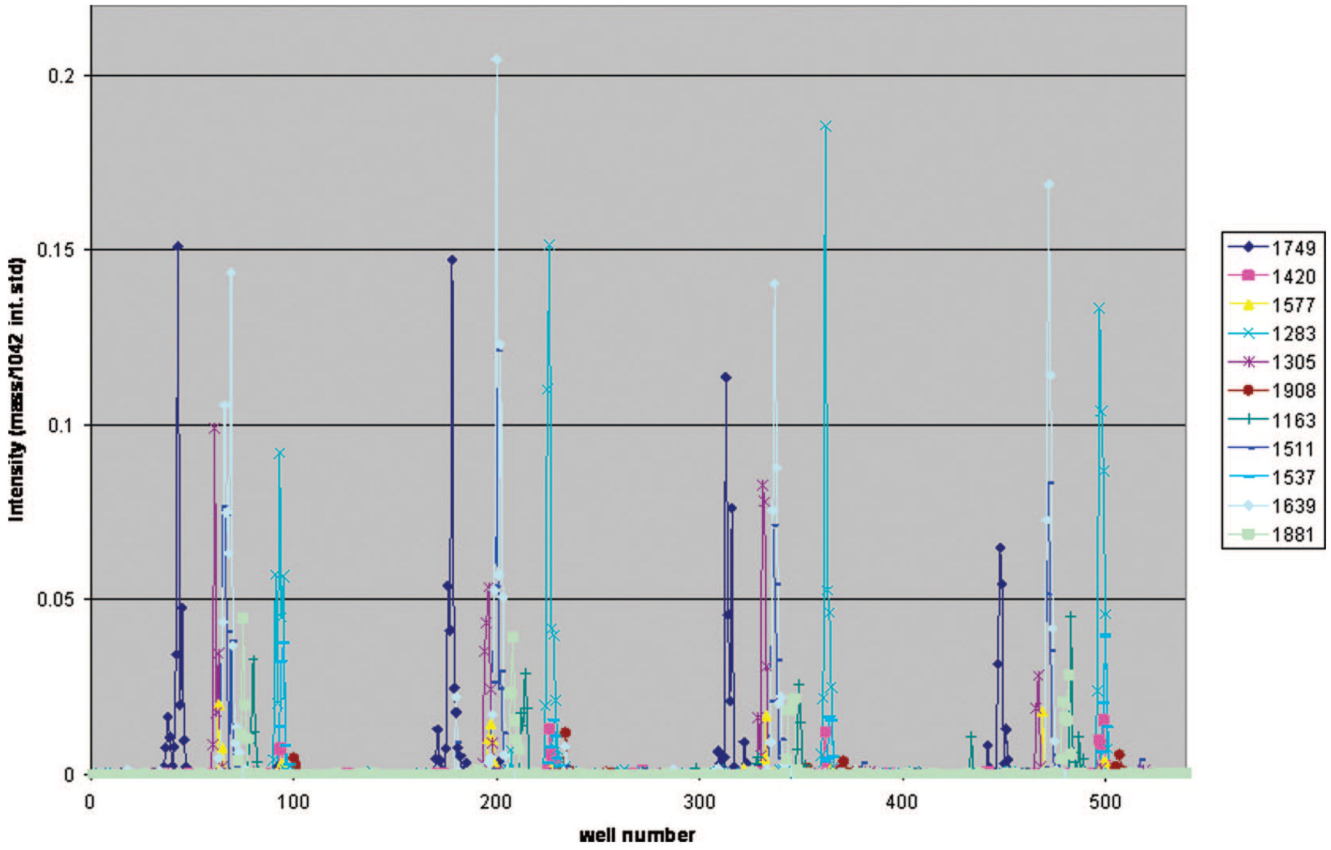

Figure 7.
Overlay of EICs from 12 peptides from four serial 50 μL/min separations of 5 pmol of BSA digest. All runs were done on a single plate, and the plot shows well number vs normalized peak intensity.

Table 1

Integrated Peak Areas from Peptides Collected from Three Identical LC Runs Performed on the Same CHS Plate

peptide mass	T1	T2	T3	average	SDRSD
927.49	19899.76	20059.38	22143.72	20700.95	1252.026.05
1163.63	4099.57	2262.48	3587.16	3316.40	948.0028.59
1305.72	5169.13	4583.40	4060.76	4604.43	554.4912.04
1439.81	11628.93	8630.20	16693.92	10129.56	2120.4220.93
1479.79	32823.71	28896.34	28739.37	28817.85	111.000.39
1567.74	44289.48	36828.69	41830.92	40983.03	3801.989.28
1639.94	14054.51	9328.95	9389.87	10924.45	2710.8924.81
1725.82	10777.22	9828.30	11405.56	9828.30	794.048.08
1881.91	11120.44	10640.06	17997.91	13252.80	4116.4031.06
1908.90	17143.60	9048.09	12614.09	13095.84	5724.3943.71
2045.03	3841.24	4964.22	5608.82	4402.73	794.0618.04
2301.08	1533.99	1178.37	1609.09	1356.18	251.4618.54
					av = 18.46

Table 2

Integrated Peak Areas from Peptides Collected from Three Identical LC Runs Performed on Different CHS Plates

peptide mass	plate 1	plate 2	plate 3	average	SDRSD
927.49	19899.76	26312.67	26109.17	24107.20	3645.1715.12
1163.63	4099.57	4444.73	6625.19	5056.50	1369.4427.08
1305.72	5169.13	4903.87	7991.75	6021.58	1711.3628.42
1479.79	32823.71	48934.72	56192.44	45983.62	11960.6126.01
1567.74	44289.48	57707.61	71577.06	64642.34	9807.1815.17
1639.94	14054.51	18424.46	23658.16	18712.38	4808.2925.70
1725.82	10777.22	9201.18	12775.68	10918.03	1791.4116.41
1881.91	11120.44	9292.27	9365.07	9925.93	1035.1210.43
1908.90	17143.60	19811.12	19143.60	18699.44	1388.127.42
2045.03	3841.24	2261.16	4033.01	3378.47	972.3628.78
2301.08	1533.99	3203.46	2829.41	2522.29	876.0934.73
					av = 21.39

Table 3

Data from Figure 4A, $N = 8$ for All Data Points

sample concn fmol	vol loaded µL	quantity loaded fmol	av signal	SD	RSD
5	5	25	51253	11128	22
5	10	50	55950	36813	66
5	15	75	59911	22681	38
50	5	250	109296	15606	14
50	10	500	135684	57009	42
50	15	750	163797	20111	12
500	5	2500	557521	153245	27
500	10	5000	594246	50070	8
500	15	7500	582918	170581	29

Table 4

Data From Figure 4B, $N = 8$ for All Data Points

sample concn fmol/μL	vol loaded μL	quantity loaded fmol	av signal	SD	RSD
5	5	25	2725	969	36
10	5	50	3145	1302	41
40	5	200	4667	1293	32
160	5	800	15355	1831	12
200	5	1000	26147	3367	13
300	5	1500	44585	2808	6
500	5	2500	112196	19333	17
1000	5	5000	175373	39432	22
1500	5	7500	287490	12519	4
2000	5	10000	232872	18492	8

Table 5

Statistical Information on the Reproducibility for Peaks Shown in Figure 6

peptide mass	av normalized intensity	SD	RSD
927.49	0.78	0.26	33.10
1163.63	0.07	0.01	16.89
1283.71	0.36	0.06	16.14
1305.72	0.15	0.07	45.47
1420.67	0.02	0.01	25.29
1479.80	0.99	0.29	29.76
1511.84	0.22	0.04	18.92
1537.74	0.05	0.01	19.81
1577.75	0.03	0.01	34.40
1639.93	0.45	0.07	16.59
1749.67	0.28	0.07	23.82
1881.91	0.09	0.00	4.14
1908.91	0.01	0.00	31.62